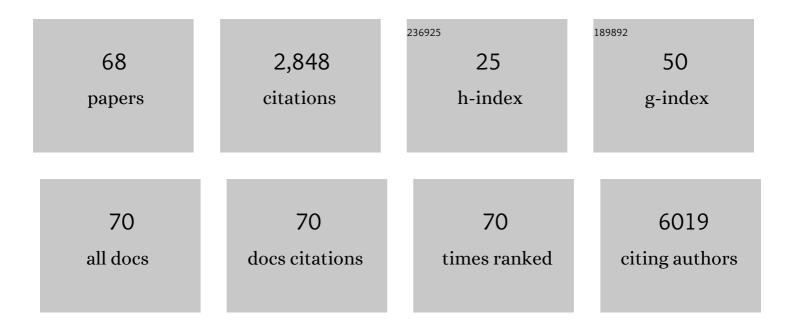
Sebastien Monette

List of Publications by Year in descending order

Source: https://exaly.com/author-pdf/8541619/publications.pdf Version: 2024-02-01



#	Article	IF	CITATIONS
1	Ultrasmall nanoparticles induce ferroptosis in nutrient-deprived cancer cells and suppress tumour growth. Nature Nanotechnology, 2016, 11, 977-985.	31.5	467
2	Surface-enhanced resonance Raman scattering nanostars for high-precision cancer imaging. Science Translational Medicine, 2015, 7, 271ra7.	12.4	236
3	Lactose drives <i>Enterococcus</i> expansion to promote graft-versus-host disease. Science, 2019, 366, 1143-1149.	12.6	217
4	Synthetic Lethal and Convergent Biological Effects of Cancer-Associated Spliceosomal Gene Mutations. Cancer Cell, 2018, 34, 225-241.e8.	16.8	162
5	The SWI/SNF Protein PBRM1 Restrains VHL-Loss-Driven Clear Cell Renal Cell Carcinoma. Cell Reports, 2017, 18, 2893-2906.	6.4	153
6	RIG-I/MAVS and STING signaling promote gut integrity during irradiation- and immune-mediated tissue injury. Science Translational Medicine, 2017, 9, .	12.4	114
7	Hematopoietic Stem Cell Origin of <i>BRAF</i> V600E Mutations in Hairy Cell Leukemia. Science Translational Medicine, 2014, 6, 238ra71.	12.4	102
8	AAVrh.10-Mediated APOE2 Central Nervous System Gene Therapy for APOE4-Associated Alzheimer's Disease. Human Gene Therapy Clinical Development, 2018, 29, 24-47.	3.1	90
9	An Atypical Parvovirus Drives Chronic Tubulointerstitial Nephropathy and Kidney Fibrosis. Cell, 2018, 175, 530-543.e24.	28.9	89
10	GNA11 Q209L Mouse Model Reveals RasGRP3 as an Essential Signaling Node in Uveal Melanoma. Cell Reports, 2018, 22, 2455-2468.	6.4	75
11	Systemic Antitumor Immunity by PD-1/PD-L1 Inhibition Is Potentiated by Vascular-Targeted Photodynamic Therapy of Primary Tumors. Clinical Cancer Research, 2018, 24, 592-599.	7.0	75
12	Fc-Mediated Anomalous Biodistribution of Therapeutic Antibodies in Immunodeficient Mouse Models. Cancer Research, 2018, 78, 1820-1832.	0.9	69
13	mTORC1 promotes cell growth via m6A-dependent mRNA degradation. Molecular Cell, 2021, 81, 2064-2075.e8.	9.7	50
14	Pathology of Aging in NOD <i>scid</i> gamma Female Mice. Veterinary Pathology, 2017, 54, 855-869.	1.7	48
15	Expression of the Carboxy-Terminal Portion of MUC16/CA125 Induces Transformation and Tumor Invasion. PLoS ONE, 2015, 10, e0126633.	2.5	41
16	ADAM10-Dependent Signaling Through Notch1 and Notch4 Controls Development of Organ-Specific Vascular Beds. Circulation Research, 2016, 119, 519-531.	4.5	39
17	Blood-induced bone loss in murine hemophilic arthropathy is prevented by blocking the iRhom2/ADAM17/TNF-Î \pm pathway. Blood, 2018, 132, 1064-1074.	1.4	38
18	Curative Multicycle Radioimmunotherapy Monitored by Quantitative SPECT/CT-Based Theranostics, Using Bispecific Antibody Pretargeting Strategy in Colorectal Cancer. Journal of Nuclear Medicine, 2017, 58, 1735-1742.	5.0	36

SEBASTIEN MONETTE

#	Article	IF	CITATIONS
19	Molecular phenotyping and image-guided surgical treatment of melanoma using spectrally distinct ultrasmall core-shell silica nanoparticles. Science Advances, 2019, 5, eaax5208.	10.3	36
20	ADAM10 controls the differentiation of the coronary arterial endothelium. Angiogenesis, 2019, 22, 237-250.	7.2	36
21	Structural modeling defines transmembrane residues in ADAM17 that are crucial for Rhbdf2/ADAM17-dependent proteolysis. Journal of Cell Science, 2017, 130, 868-878.	2.0	34
22	Preclinical ⁸⁹ Zr Immuno-PET of High-Grade Serous Ovarian Cancer and Lymph Node Metastasis. Journal of Nuclear Medicine, 2016, 57, 771-776.	5.0	31
23	Glomerular endothelial cell maturation depends on ADAM10, a key regulator of Notch signaling. Angiogenesis, 2018, 21, 335-347.	7.2	31
24	Intraoperative Ultrasound and Tissue Elastography Measurements Do Not Predict the Size of Hepatic Microwave Ablations. Academic Radiology, 2014, 21, 72-78.	2.5	30
25	Feasibility of Catheter-Directed Intraluminal Irreversible Electroporation of Porcine Ureter and Acute Outcomes in Response to Increasing Energy Delivery. Journal of Vascular and Interventional Radiology, 2015, 26, 1059-1066.	0.5	28
26	Alpha radioimmunotherapy using ²²⁵ Ac-proteus-DOTA for solid tumors - safety at curative doses. Theranostics, 2020, 10, 11359-11375.	10.0	26
27	Alloreactive T cells deficient of the short-chain fatty acid receptor GPR109A induce less graft-versus-host disease. Blood, 2022, 139, 2392-2405.	1.4	24
28	Nonthermal Ablation by Using Intravascular Oxygen Radical Generation with WST11: Dynamic Tissue Effects and Implications for Focal Therapy. Radiology, 2016, 281, 109-118.	7.3	23
29	Murine and related chapparvoviruses are nephro-tropic and produce novel accessory proteins in infected kidneys. PLoS Pathogens, 2020, 16, e1008262.	4.7	23
30	Prognostic Indicators and Clinical Outcome in Dogs with Subcutaneous Mast Cell Tumors Treated with Surgery Alone: 43 Cases. Journal of the American Animal Hospital Association, 2020, 56, 215-225.	1.1	21
31	Transmural ablation of the normal porcine common bile duct with catheter-directed irreversible electroporation is feasible and does not affect duct patency. Gastrointestinal Endoscopy, 2018, 87, 300.e1-300.e6.	1.0	20
32	Normal Porcine Ureter Retains Lumen Wall Integrity but Not Patency Following Catheter-Directed Irreversible Electroporation: Imaging and Histologic Assessment over 28 Days. Journal of Vascular and Interventional Radiology, 2017, 28, 913-919.e1.	0.5	19
33	Androgen Deprivation Therapy Potentiates the Efficacy of Vascular Targeted Photodynamic Therapy of Prostate Cancer Xenografts. Clinical Cancer Research, 2018, 24, 2408-2416.	7.0	19
34	Induction and characterization of pancreatic cancer in a transgenic pig model. PLoS ONE, 2020, 15, e0239391.	2.5	19
35	A Self-Assembling and Disassembling (SADA) Bispecific Antibody (BsAb) Platform for Curative Two-step Pretargeted Radioimmunotherapy. Clinical Cancer Research, 2021, 27, 532-541.	7.0	19
36	MRI-guided focused ultrasound ablation of lumbar medial branch nerve: Feasibility and safety study in a swine model. International Journal of Hyperthermia, 2016, 32, 786-794.	2.5	18

#	Article	IF	CITATIONS
37	Treatment Effects of WST11 Vascular Targeted Photodynamic Therapy for Urothelial Cell Carcinoma in Swine. Journal of Urology, 2016, 196, 236-243.	0.4	18
38	An apoptosis-dependent checkpoint for autoimmunity in memory B and plasma cells. Proceedings of the United States of America, 2020, 117, 24957-24963.	7.1	18
39	Carbon nanotubes exhibit fibrillar pharmacology in primates. PLoS ONE, 2017, 12, e0183902.	2.5	18
40	CD19-directed chimeric antigen receptor T cell therapy in Waldenström macroglobulinemia: a preclinical model and initial clinical experience. , 2022, 10, e004128.		18
41	Oncolytic herpes simplex virus kills stem-like tumor-initiating colon cancer cells. Molecular Therapy - Oncolytics, 2016, 3, 16013.	4.4	16
42	Pleural Puncture that Excludes the Ablation Zone Decreases the Risk of Pneumothorax after Percutaneous Microwave Ablation in Porcine Lung. Journal of Vascular and Interventional Radiology, 2015, 26, 1052-1058.	0.5	14
43	High power microwave ablation of normal swine lung: impact of duration of energy delivery on adverse event and heat sink effects. International Journal of Hyperthermia, 2018, 34, 1186-1193.	2.5	14
44	Transarterial Embolization of Liver Cancer in a Transgenic Pig Model. Journal of Vascular and Interventional Radiology, 2021, 32, 510-517.e3.	0.5	14
45	Catheter-based endobronchial electroporation is feasible for the focal treatment of peribronchial tumors. Journal of Thoracic and Cardiovascular Surgery, 2018, 155, 2150-2159.e3.	0.8	13
46	Developmental and behavioral effects of toe clipping on neonatal and preweanling mice with and without vapocoolant anesthesia. Journal of the American Association for Laboratory Animal Science, 2014, 53, 132-40.	1.2	13
47	Interferon regulatory factor 2 protects mice from lethal viral neuroinvasion. Journal of Experimental Medicine, 2016, 213, 2931-2947.	8.5	12
48	In Vivo Imaging With Confirmation by Histopathology for Increased Rigor and Reproducibility in Translational Research: A Review of Examples, Options, and Resources. ILAR Journal, 2018, 59, 80-98.	1.8	12
49	Ultrasmall Nanoparticle Delivery of Doxorubicin Improves Therapeutic Index for High-Grade Glioma. Clinical Cancer Research, 2022, 28, 2938-2952.	7.0	11
50	Ablation of the sacroiliac joint using MR-guided high intensity focused ultrasound: a preliminary experiment in a swine model. Journal of Therapeutic Ultrasound, 2017, 5, 17.	2.2	10
51	Caveolin-1 temporal modulation enhances antibody drug efficacy in heterogeneous gastric cancer. Nature Communications, 2022, 13, 2526.	12.8	10
52	Targeted truncation of the ADAM17 cytoplasmic domain in mice results in protein destabilization and a hypomorphic phenotype. Journal of Biological Chemistry, 2021, 296, 100733.	3.4	9
53	Effects of Breeding Configuration on Maternal and Weanling Behavior in Laboratory Mice. Journal of the American Association for Laboratory Animal Science, 2017, 56, 369-376.	1.2	8
54	Reemergence of the Murine Bacterial Pathogen <i>Chlamydia muridarum</i> in Research Mouse Colonies. Comparative Medicine, 2022, 72, 230-242.	1.0	7

#	Article	IF	CITATIONS
55	The potential risk of tumor progression after use of dehydrated human amnion/chorion membrane allograft in a positive margin resection model. Therapeutic Advances in Urology, 2019, 11, 175628721983777.	2.0	6
56	Engineered Cells as a Test Platform for Radiohaptens in Pretargeted Imaging and Radioimmunotherapy Applications. Bioconjugate Chemistry, 2021, 32, 649-654.	3.6	6
57	A Novel α-Hemolytic Streptococcus Species (Streptococcus azizii sp. nov.) Associated with Meningoencephalitis in NaÃ ⁻ ve Weanling C57BL/6 Mice. Comparative Medicine, 2015, 65, 186-95.	1.0	6
58	Intraperitoneal Pretargeted Radioimmunotherapy for Colorectal Peritoneal Carcinomatosis. Molecular Cancer Therapeutics, 2022, 21, 125-137.	4.1	5
59	Phenotypic and molecular states of IDH1 mutation-induced CD24-positive glioma stem-like cells. Neoplasia, 2022, 28, 100790.	5.3	5
60	Positron Emission Tomography/Computed Tomography with Gallium-68–labeled Prostate-specific Membrane Antigen Detects Relapse After Vascular-targeted Photodynamic Therapy in a Prostate Cancer Model. European Urology Focus, 2021, 7, 472-478.	3.1	4
61	Neoadjuvant vascular-targeted photodynamic therapy improves survival and reduces recurrence and progression in a mouse model of urothelial cancer. Scientific Reports, 2021, 11, 4842.	3.3	4
62	Ultrasound-Guided Percutaneous Laser Ablation of the Thyroid Gland in a Swine Model: Comparison of Ablation Parameters and Ablation Zone Dimensions CardioVascular and Interventional Radiology, 2021, 44, 1798-1806.	2.0	4
63	Disseminated coelomic xanthogranulomatosis in eclectus parrots (<i>Eclectus roratus</i>) and budgerigars (<i>Melopsittacus undulatus</i>). Veterinary Pathology, 2022, 59, 143-151.	1.7	4
64	Feasibility of a Modified Biopsy Needle for Irreversible Electroporation Ablation and Periprocedural Tissue Sampling. Technology in Cancer Research and Treatment, 2016, 15, 749-758.	1.9	3
65	Chaphamaparvovirus antigen and nucleic acids are not detected in kidney tissues from cats with chronic renal disease or immunocompromised cats. Veterinary Pathology, 2022, 59, 120-126.	1.7	3
66	Augmented fluoroscopy guided transbronchial pulmonary microwave ablation using a steerable sheath. Translational Lung Cancer Research, 2022, 11, 150-164.	2.8	3
67	Abstract No. 617 Nonthermal ablation of pancreatic cancer in a pig model, using vascular-targeted photodynamic therapy (VTP). Journal of Vascular and Interventional Radiology, 2019, 30, S266.	0.5	1
68	Abstract 15364: Radiation Exposure of the Base of the Heart Accelerates Coronary Atherosclerosis. Circulation, 2020, 142, .	1.6	1